

One-Pot Synthesis of 1,3,5-Trisubstituted Pyrazoles via Immobilized *Thermomyces lanuginosus* Lipase (TLL) on a Metal–Organic Framework

Zeynab Rangraz, Mostafa M. Amini, and Zohreh Habibi*



Cite This: *ACS Omega* 2024, 9, 19089–19098



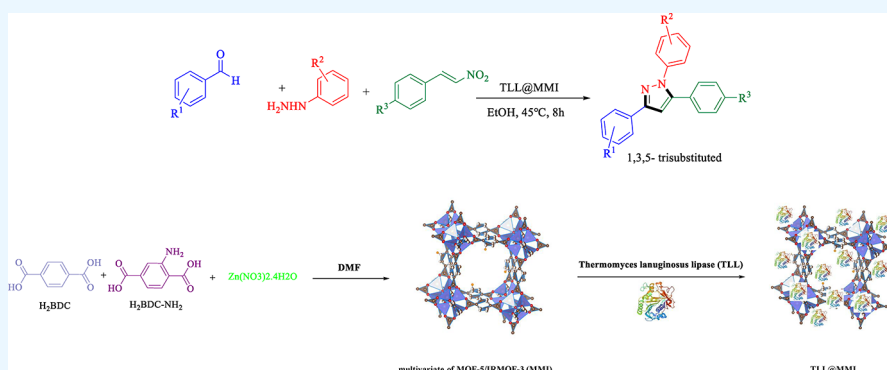
Read Online

ACCESS |

Metrics & More

Article Recommendations

Supporting Information



ABSTRACT: A regioselective enzyme-catalyzed system is selected for the synthesis of 1,3,5-trisubstituted pyrazole derivatives by adding phenyl hydrazines, nitroolefins, and benzaldehydes. The reaction is performed in a one-pot vessel with a yield ranging from 49 to 90%. TLL@MMI, immobilized *Thermomyces lanuginosus* lipase (TLL) on a multivariate of MOF-5/IRMOF-3 (MMI), showed good performance for the catalysis of this reaction. The prepared biocatalyst was characterized by FTIR, XRD, SEM, and EDX. The thermal and solvent stability of TLL@MMI was investigated in MeOH and EtOH after 24 h incubation. In the presence of 100% concentrations of EtOH, TLL@MMI has 80% activity.

1. INTRODUCTION

Pyrazoles are five-membered rings containing two adjacent nitrogens,¹ which are present in the structure of many drugs such as celecoxib, lonazolac, difenamizole, SC-560, and CDPPB^{2–6} (Figure 1). Pyrazoles, due to their biological and pharmacological activities such as antifungal, antiviral, anticancer, antioxidant, antibacterial, and anti-inflammatory, have been the subject of many studies.^{7–11} Due to the high importance of pyrazole in the pharmaceutical industry, providing green synthetic methods for pyrazole has always been of interest.^{12–14}

Multicomponent reactions (MCRs) are an effective, fast, and influential method that has been used in the synthesis of organic compounds since 1850.¹⁵ The absence of the need to purify the intermediates in each step of the reaction is one of the features of this method, which saves time and money. MCRs generally include addition of more than two starting materials along with all the reagents and catalysts in the same container at the same time to produce the final product.¹⁶ This synthetic method has been used in various fields, including medicinal, polymer, and agricultural chemistry. It is estimated that almost 5% of the available drugs are produced by this method.¹⁷

Until now, various methods for the synthesis of pyrazole and its derivatives have been reported. By using hydrazonoyl

chlorides and cinnamic aldehydes in two steps, derivatives of 1,3,5-trisubstituted pyrazole were synthesized (Figure 2, line 1).¹⁸ The combination of hydrazones and α -bromo ketones under visible-light catalysis led to the synthesis of 1,3,5-trisubstituted pyrazoles (Figure 2, line 2).¹⁹ N-monosubstituted hydrazones and nitroolefins are used to synthesize 1,3,5-trisubstituted pyrazoles, which without a catalyst take a long duration (1–4 days). Some derivatives were synthesized at room temperature, others under reflux conditions (Figure 2, line 3).²⁰ Also, the copper catalyst was used for the synthesis of derivatives of 1,3,4-trisubstituted pyrazole by [3+2] cycloaddition (Figure 2, line 4).²¹ One-pot three component reaction with hydrazine, nitroolefin, and aldehydes also reported 1,3,4-trisubstituted pyrazole synthesis, but the reaction in the presence of different substitutes has not been investigated (Figure 2, line 5).²²

Received: December 11, 2023

Revised: April 4, 2024

Accepted: April 8, 2024

Published: April 17, 2024



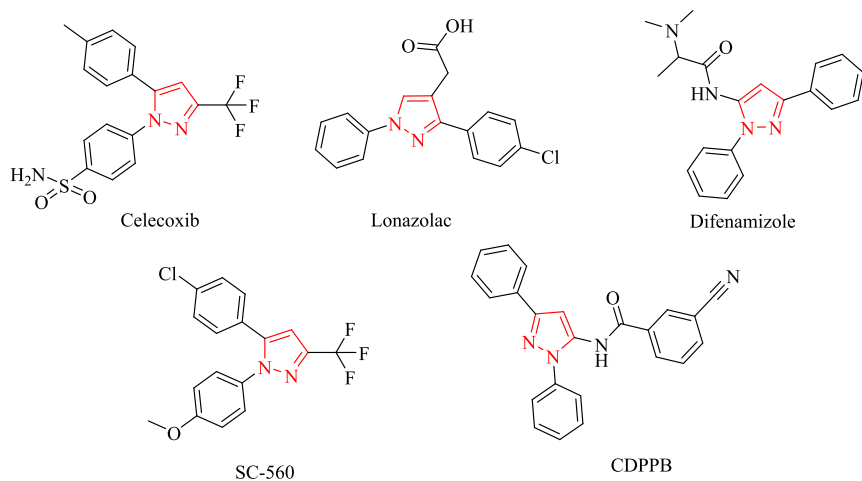
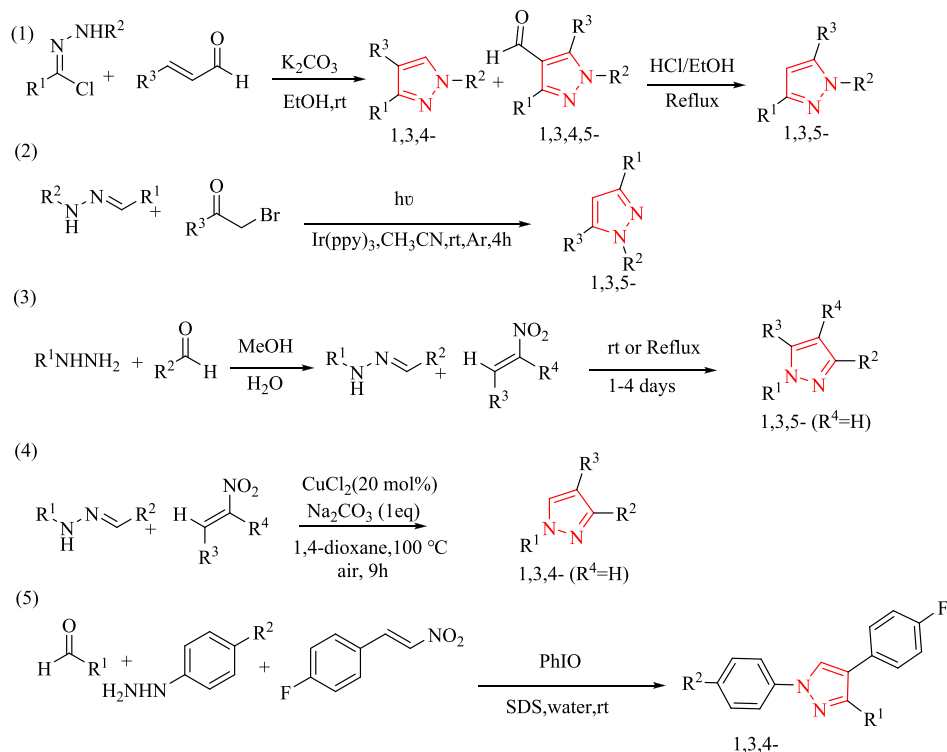


Figure 1. Some Examples of Bioactive Compounds Containing Pyrazole.

previous works:



This work:

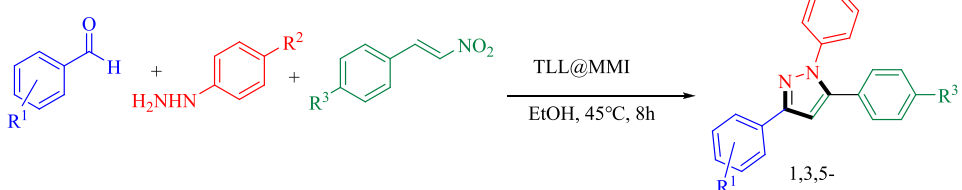


Figure 2. Various methods for the synthesis of pyrazole.

Enzyme is a green catalyst that performs reactions with high specificity and speed.²³ Enzymes are used as catalysts in various industries such as pharmaceuticals, biosensors, and food.²⁴ However, enzymes have low resistance to high temperatures, organic solvents, and very acidic or basic pH levels.^{25,26}

Considering the high costs of purifying enzymes, it seems that their use is not cost-effective due to their high sensitivity. However, there are various ways to fix enzyme problems. One of these methods is enzyme immobilization.^{27,28} Porous substrate is one of the most widely used platforms for enzyme

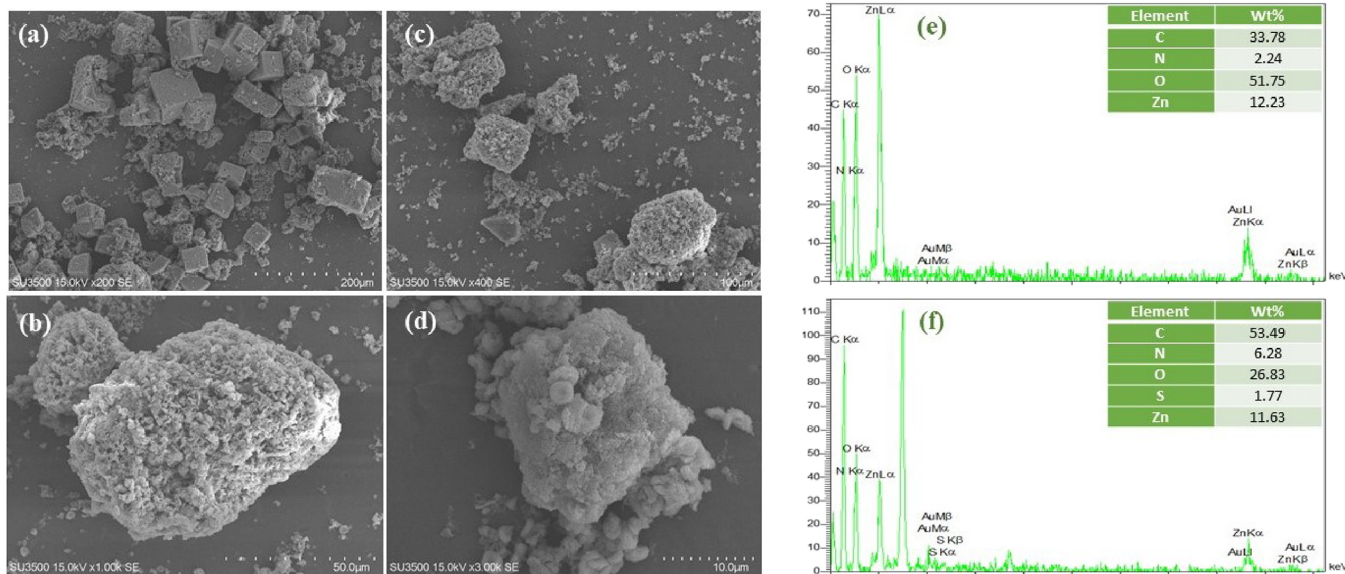


Figure 3. SEM images of MMI (a), TLL@MMI (b), and TLL@MMI after use in pyrazole synthesis (c, d). EDX analyses of MMI (e) and TLL@MMI (f).

immobilization. Silica, organic microparticles, and metal–organic frameworks (MOFs) are an example of these platforms.^{29–31} MOFs consist of metal cores and organic ligands, and due to their high active surface, adjustable cavities, and resistance to high temperature and chemicals, they are a suitable substrate for enzyme immobilization.^{32,33}

In recent years, enzymes have been used as a powerful method in synthesis of organic compounds.³⁴ Enzyme promiscuity in chemical reactions has been one of the fascinating debates about enzymes.³⁵ Lipases normally catalyze three types of reactions: hydrolysis, esterification, and transesterification. Due to reports in the literature about unusual lipase reactions, lipase promiscuity has been noticed.³⁶ Lipase has been used as a catalyst in important organic reactions such as the Canizzaro reaction, Manich reaction, aldol condensation, Baylis–Hillman reaction, Hantzsch reaction, Knoevenagel condensation, Ugi, Michael addition, Biginell reaction, and Pudovic–Abramov reaction.^{37–41}

Herein, we succeeded in synthesizing pyrazole using immobilized *Thermomyces lanuginosus* lipase (TLL) on a metal–organic framework (MOF) substrate, which we prepared in our earlier study. In that work, we successfully immobilized *T. lanuginosus* lipase (TLL) on multivariate of MOF-5/IRMOF-3 (MMI) that have a half amino group (–NH₂) and used them in synthesizing thiazole derivatives. The purpose of this immobilization was to investigate the effect of the amine group (–NH₂) on enzyme immobilization. Based on the results obtained, the immobilized enzyme was almost 2.5-fold more active than the free enzyme. When the number of amino groups decreased (in the MOF structure), the activity increased. Three MOFs (metal–organic framework-5 (MOF-5), isoreticular metal–organic frameworks-3 (IRMOF-3), and multivariate of MOF-5/IRMOF-3 (MMI) that have a half amino group (–NH₂) were used to investigate the effect of the amine group. The activity of TLL@MOF-5, TLL@IRMOF-3, and TLL@MMI was 55, 75, and 110 U/mg, respectively. In that work, the enzyme is only attached to the MOF using surface bonds, and this can reduce the complete stability of the biocomposite. However, because the purpose of that work was to investigate the effect of the

amine group, no further attempts were made to stabilize the immobilized enzyme. This problem can be investigated in future works, and the weakness of this immobilization can be solved. In this study, to show the stability and ability of this biocatalyst with all its weaknesses, we presented another synthesis for this biocatalyst (without any change in the biocatalyst preparation method). Also, the stability of TLL@MMI at high concentration of organic solvents was investigated to show that this biocatalyst has a high ability in the synthesis of organic compounds.

Accordingly, for the first time, we synthesized 1,3,5-trisubstituted pyrazoles through a one-pot three-component reaction (phenyl hydrazines, nitroolefins, and benzaldehydes) by TLL@MMI as a catalyst in mild conditions.

2. MATERIALS AND METHODS

2.1. Materials. *T. lanuginosus* lipase (TLL) and phenacyl bromides were purchased from Sigma-Aldrich. Zinc nitrate tetrahydrate (Zn(NO₃)₂·4H₂O), terephthalic acid (H₂BDC), 2-aminoterephthalic acid, and aldehydes were purchased from Merck Co.

2.2. Characterization. The scanning electron microscope (SEM), SU3500, was used to determine the surface morphology of MMI and TLL@MMI. The constituent elements of MMI and TLL@MMI were analyzed by an energy-dispersive X-ray (EDX) instrument in conjunction with the SEM. The X-ray diffraction (XRD) spectra of MMI, TLL@MMI, and TLL@MMI after using were analyzed (scintillation counter) with Cu radiation ($\lambda = 1.5406 \text{ \AA}$). Fourier transform infrared spectroscopy (FTIR) with Bruker Equinox 55 from a wavenumber of 600 to 3800 cm⁻¹ was used to analyze TLL, TLL@MMI, and TLL@MMI after using.

2.3. Preparation of MMI. MTV-MOF-5/IRMOF-3(MMI) was prepared by a mixture of 2-aminoterephthalic acid and H₂BDC by the solvothermal method.^{42,43} 2-Aminoterephthalic acid (0.137 g), H₂BDC (0.208 g), and Zn(NO₃)₂·4H₂O (1.56 g) were dissolved in 75 mL of DMF and then transferred to a Teflon reactor and kept at 105 °C for 21 h. The mixture was cooled down to room temperature. Then, the product was separated by centrifugation. The obtained crystal was washed

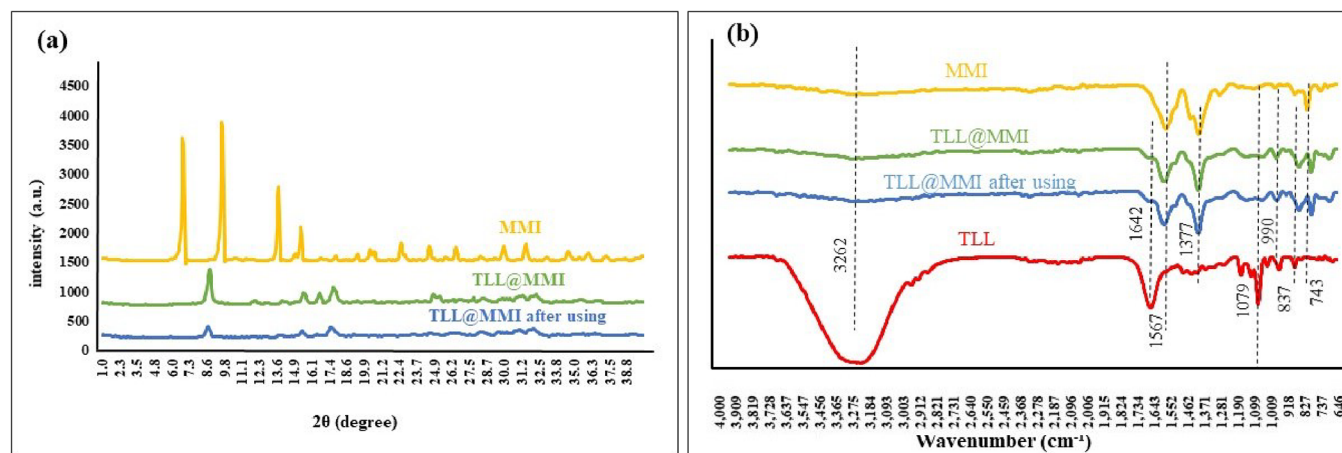


Figure 4. (a) XRD patterns of MMI, TLL@MMI, and TLL@MMI after using one cycle in the synthesis of pyrazole. (b) FTIR spectra of MMI, TLL@MMI, free TLL, and TLL@MMI after using one cycle in the synthesis of pyrazole.

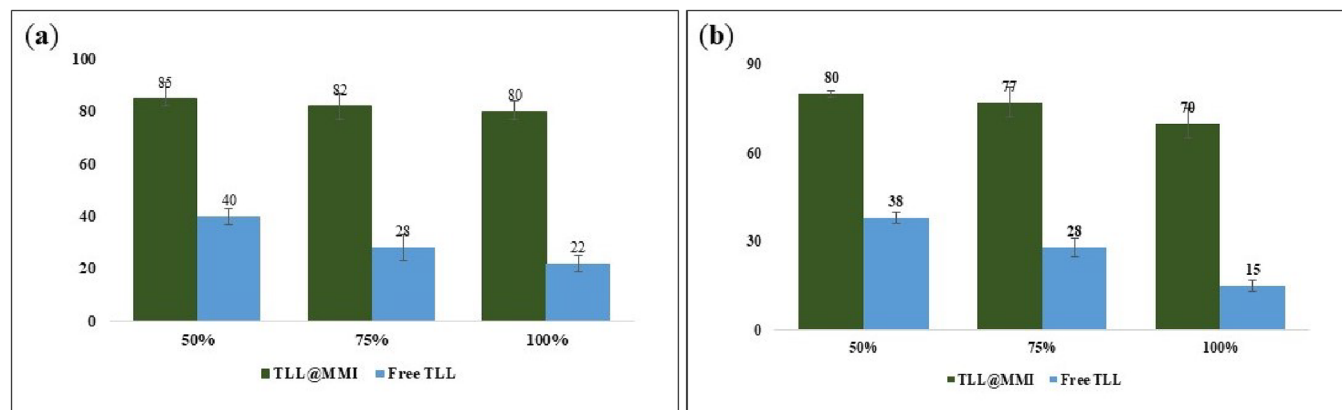


Figure 5. Solvent stability of TLL@MMI and free TLL. (a) Solvent stability of TLL@MMI and free TLL in 50, 75, and 100% of EtOH. (b) Solvent stability of TLL@MMI and free TLL 50, 75, and 100% of MeOH. Experimental conditions: 10 mg of immobilized enzyme was dispersed in 20 mL of potassium phosphate buffer 10 mM pH 7.2 and then incubated for 24 h in different amounts of solvents.

three times with DMF. Then, it was soaked in MeOH about 7 days (MeOH was changed every 2 days). The crystals were divided from MeOH and dried 3 h at 100 °C in the oven.

2.4. Preparation of TLL@MMI. TLL@MMI was prepared by adding 1.5 mg (100 μL) of TLL (16 mg/mL) to 10 mg of MMI. It was stirred at 15–20 °C in 200 rpm for 24 h. Then, TLL@MMI was centrifuged and washed three times with potassium phosphate buffer, at pH 7.2. Finally, it was dried with a vacuum system at room temperature for 3 h.

2.5. Activity Assay of Free and Immobilized TLL. Free and immobilized TLL activity was calculated by changing the amount of *p*-nitrophenol during the *p*-nitrophenyl butyrate (*p*-NPB) hydrolysis in 10 mM potassium phosphate buffer at pH 8.2 and 25 °C. To measure the activity of free TLL, 20 μL of CAL-B was dissolved in 12 mL of potassium phosphate buffer 10 mM pH 7.2. Then, 20 μL of this solution was added to 2 mL of potassium phosphate buffer 10 mM pH 8.2 that contained 20 μL of *p*-NPB 30 mM. After that, absorbance change was measured over 2 min at 410 nm ($\epsilon = 17500 \text{ M}^{-1}\text{cm}^{-1}$). To measure the activity of the immobilized enzyme, 2 mg of TLL@MMI was added to 10 mL of phosphate buffer 10 mM pH 7.2 and then 20 μL of this suspension was added to 2 mL of potassium phosphate buffer 10 mM pH 8.2 and 20 μL of *p*-NPB 30 mM. Then, the activity of immobilized TLL was calculated by the *p*-NPB assay.

2.6. Thermal Stability in Organic Solvents. In order to measure the thermal stability of the immobilized TLL, free and immobilized TLL were incubated in MeOH and EtOH at 45 °C for 24 h; their activities were measured by the *p*-NPB assay.

2.7. Stability in Organic Solvents. To determine the stability of TLL@MMI in organic solvents, free and immobilized TLL were incubated in 1 mL of solution containing 50, 75, and 100% (v/v) of MeOH and EtOH at room temperature during 24 h.

2.8. Reusability of TLL@MMI. To investigate the reusability of TLL@MMI, after the reaction, the biocatalyst was separated from the reaction mixture. The mixture was dissolved in the excess amount of ethanol, and then it was centrifuged to separate the catalyst. The separated biocatalyst was washed three times with ethanol and potassium buffer pH 8.5 and then dried under vacuum. The activity of the recovered biocatalyst was measured by the *p*-NPB assay and then reused in reaction. All of the steps were repeated five times.

3. RESULTS AND DISCUSSION

3.1. Characterization of Cu-BTC and CAL-B@Cu-BTC. SEM and EDX Analyses. The appearance of the MMI is cubic,^{42,43} which is well represented in the SEM image (Figure 3). After enzyme immobilization, due to enzyme coating on the surface of the MOF, the cubic structure has changed slightly.

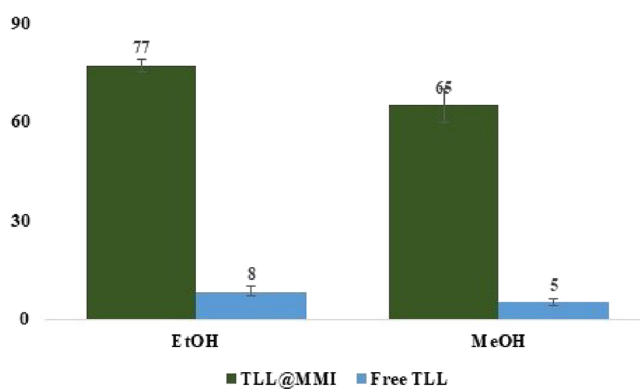


Figure 6. Thermal stability of TLL@MMI and free TLL in EtOH and MeOH at 45 °C. Experimental conditions: 1 mg of immobilized enzyme was dispersed in 1 mL of solvent and then incubated for 24 h at 45 °C.

The EDX analysis was used to prove the addition of the enzyme. MMI contains Zn, C, N, and O elements (Figure 3e). The appearance of S and the increasing the amount of N in the EDX of TLL@MMI indicated the presence of the enzyme in the composite.

XRD Analysis. The XRD spectra of MMI, TLL@MMI, and TLL@MMI after using were analyzed (Figure 4a). Strong diffraction peaks at 2-theta of 6.6, 9.4, and 13.5° are consistent with previous reports.^{42,43} According to previous works,^{44–46} when a substance is loaded on the MOF surface, there is a possibility of shifting the XRD peaks. According to the SEM image and the high amount of enzyme, this is likely to happen and it is probably due to a decrease in the crystalline nature of the MOF.

FTIR Analysis. FTIR of TLL, TLL@MMI, MMI, and TLL@MMI after using in pyrazole synthesis was conducted at a wavenumber of 600–3800 cm⁻¹ (Figure 4b). Although the XRD pattern after enzyme immobilization has a slight shift, FTIR shows the formation of MOF bonds before and after enzyme immobilization. The fingerprint of terephthalate was assigned at 1200–600 cm⁻¹, and the vibration of BDC was assigned at 1606–1505 and 1400–1256 cm⁻¹.⁴⁷

3.2. Effect of Solvent on the Activity of Free TLL and TLL@MMI. A suitable biocatalyst or catalyst must show proper stability in various solvents; therefore, their stability in solvents must be investigated.^{48,49} To determine the solvent stability of

TLL@MMI, EtOH and MeOH (used in synthetic reactions) were chosen. Free TLL and TLL@MMI were incubated in a mixture of 50, 75, and 100% (v/v) of EtOH and MeOH for 24 h (Figure 5a,b). In all cases, TLL@MMI exhibited more activity than the free TLL. In a mixture of 50, 75, and 100% (v/v) of EtOH, TLL@MMI has more than 80% activity while the free TLL has lost more than 60% activity. In a mixture of 100% (v/v) MeOH, free TLL has 15% activity while TLL@MMI has 70% activity. In the best situation, in a mixture of 100% (v/v) of EtOH, TLL@MMI has 80% activity.

3.3. Effect of Temperature on the Activity of Free TLL

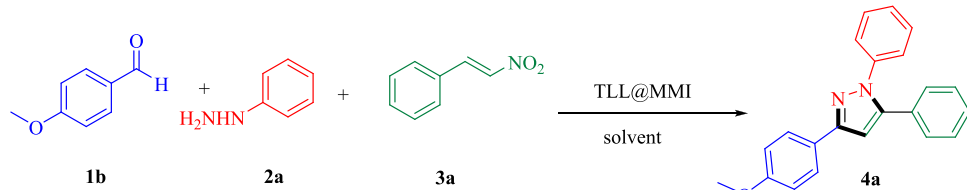
and TLL@MMI. In previous reports, the immobilized enzyme has a thermal stability higher than that of the free enzyme. This test is usually done using a buffer.^{50,51} Herein, to show the stability of the immobilized enzyme, thermal stability of the immobilized enzyme was performed after 24 h of incubation of the free TLL and TLL@MMI at 45 °C in EtOH and MeOH (Figure 6). After 24 h of incubation, free TLL is almost inactive in both solvents, but TLL@MMI has 77 and 65% activity in EtOH and MeOH, respectively.

3.4. Pyrazole Synthesis. As mentioned in the introduction, pyrazole is a widely used substance in medicines. Therefore, many efforts are being made to prepare this structure in a green environment. On this basis, we presented a method for the synthesis of pyrazole using an enzyme that is a green catalyst. For this purpose, commercially available lipase enzymes and immobilized lipase enzymes were used.

At first, to explore the best conditions for the reaction, different solvents, temperature, time, and amount of catalyst were investigated. The highest efficiency was obtained from the reaction of benzaldehyde **1** (1 mmol), phenyl hydrazine hydrochloride **2a** (1 mmol), and niroolefine **3a** (1 mmol) at 45 °C in ethanol as a solvent and 10 mg of TLL@MMI in 8 h.

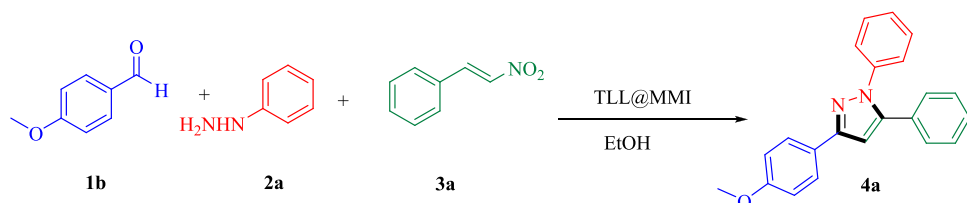
In detail, five solvents were selected (Table 1), among which EtOH had the highest efficiency (Table 1, entry 3), and in the presence of DMF, the efficiency was less than 10% (Table 1, entry 5). In continuation of the optimization path, EtOH was used as a solvent. Then, the reaction was carried out at different temperatures for 24 h. Temperatures from 25 to 55 °C were investigated (Table 2). An efficiency of higher than 73% was observed in all temperatures; among them, the temperature of 45 °C showed the best performance with 83% yield (Table 2, entry 3). At the temperature of 45 °C, the yield of the reaction was controlled from 5 to 24 h (Table 2, entries 5–7); after 8 h

Table 1. Screening of a Suitable Solvent^a



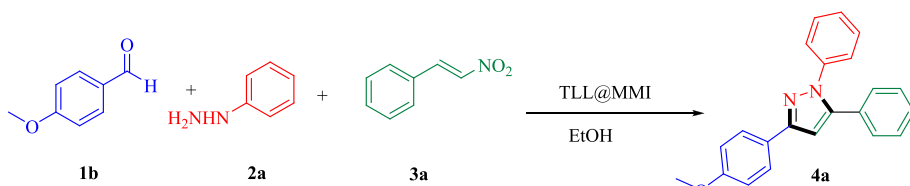
entry	solvent	temperature (°C)	time (h)	yield (%)
1	H ₂ O	25	24	41
2	buffer phosphate pH 8	25	24	46
3	EtOH	25	24	73
4	MeOH	25	24	58
5	DMF	25	24	trace

^aReagents and conditions: 4-methoxy benzaldehyde **1b** (1 mmol), phenyl hydrazine hydrochloride **2a** (1 mmol), β -nitrostyrene **3a** (1 mmol), TLL@MMI (10 mg), and solvent (2 mL).

Table 2. Screening of the Suitable Temperature and Reaction Time^a

entry	time (h)	temperature (°C)	yield (%)
1	24	25	73
2	24	35	78
3	24	45	83
4	24	55	80
5	5	45	69
6	8	45	83
7	12	45	83

^aReagents and conditions: 4-methoxy benzaldehyde **1b** (1 mmol), phenyl hydrazine hydrochloride **2a** (1 mmol), β -nitrostyrene **3a** (1 mmol), TLL@MMI (10 mg), and EtOH (2 mL).

Table 3. Effect of the Amount of Catalyst

entry	temperature (°C)	time (h)	amount of catalyst (mg)	yield (%)
1	45	24	5	66
2	45	24	10	83
3	45	24	15	79
4	45	24	20	63

^aReagents and conditions: 4-methoxy benzaldehyde **1b** (1 mmol), phenyl hydrazine hydrochloride **2a** (1 mmol), β -nitrostyrene **3a** (1 mmol), TLL@MMI (10 mg), and EtOH (2 mL).

Table 4. Screening of Different Catalysts^a

entry	catalyst	amount of catalyst (mg)	time	yield (%)
1	no enzyme		3 days	trace
2	porcine pancreas lipase (PPL)	10	24 h	10
3	<i>Thermomyces lanuginosus</i> lipase (TLL)	10 ^b	24 h	21
4	Novozym 435	10	24 h	42
5	TLL@MMI	10 ^c	24 h	73
6	bovine serum albumin (BSA)	10	24 h	trace
7	MMI	10	24 h	20
8	IRMOF-3	10	24 h	15

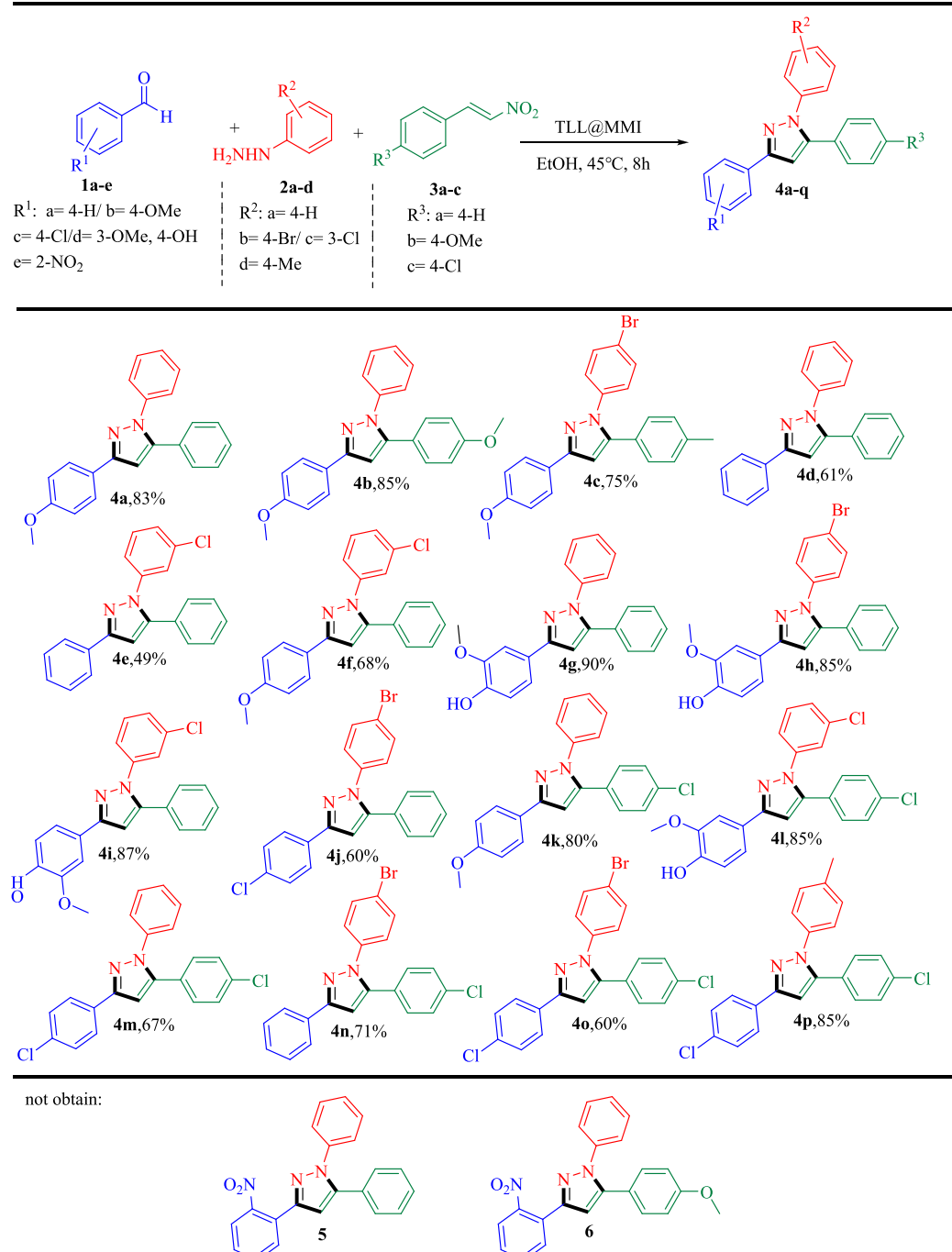
^aReagents and conditions: 4-methoxy benzaldehyde **1b** (1 mmol), phenyl hydrazine hydrochloride **2a** (1 mmol), β -nitrostyrene **3a** (1 mmol), temperature (25 °C), and EtOH (2 mL). ^b625 μ L of TLL. ^c10 mg of catalyst contain 1.15 mg of TLL.

from the start of the reaction, the yield of the reaction did not increase, so 8 h was chosen as the best time (Table 2, entry 6). In the end, different amounts of catalyst were used (Table 3), and when the amount of catalyst exceeded 10 mg, the yield of the reaction decreased. Therefore, the highest yield was obtained using 10 mg of catalyst for 1 mmol of starting materials (Table 3, entry 2).

Other catalysts were used to compare the performance of TLL@MMI (Table 4). After TLL@MMI with a yield of 73% (Table 4, entry 5), Novozym 435 showed the highest yield (Table 4, entry 4, with a 42% yield). Furthermore, isoreticular metal–organic frameworks-3 (IRMOF-3) and multivariate MOF-5/IRMOF-3 (MMI) were used as catalysts to ensure the effect of MOFs in this reaction, which had an efficiency of less than 20% (Table 4, entries 7 and 8).

To investigate the diversity of the reaction, benzaldehyde **1a–e**, phenyl hydrazine hydrochloride **2a–d**, and β -nitrostyrene **3a–c** were reacted under the optimum conditions to obtain 1,3,5-trisubstituted pyrazole **4a–p** in different yields ((49–90%, Scheme 1). Among the derivatives made, the yield increased when electron-donating benzaldehydes and electron-withdrawing-substituted benzaldehydes reduced the yield. Compounds **4a**, **4b**, **4g**, **4h**, **4i**, **4l**, and **4p** have yields of more than 83%. When a nitro group was substituted in the *ortho* position, compounds **5** and **6** were not obtained (Scheme 1).

Deng and Mani in 2006 reported the reaction mechanism between 1,3-dipolar and nitroolefins as [3+2] cycloaddition.²⁰ However, after 2 years, they reached a single product using *cis*- and *trans*-nitroolefin isomers and concluded that the path of this reaction does not go through concerted cycloaddition.⁵² Based on the mechanisms related to lipase^{53,54} and according to the step mechanism of Deng and Mani, the proposed mechanism was presented (Scheme 2). First, imine intermediate **7** forms

Scheme 1. TLL@MMI-Catalyzed 1,3,5-Trisubstituted Pyrazole Derivatives (4a–q)^a

^aReagents and conditions: benzaldehydes 1a–e (1 mmol), phenyl hydrazine hydrochlorides 2a–d (1 mmol), β -nitrostyrenes 3a–c (1 mmol), TLL@MMI (10 mg), EtOH (2 mL), and temperature (45 °C).

from the reaction of phenyl hydrazine 2 with aldehyde 1 and then Asp-His dyad 13 activates nitrogen. Intermediate 7 adds to the nitroolefin 8, so that the NO_2 group stabilizes by an oxyanion hole. Intramolecular cyclization occurs with the transfer of protons from enzyme 14 to intermediate 9. Finally, 1,3,5-trisubstituted pyrazole 4 forms by oxidizing the ring and removing HNO_2 .

3.6. Reusability. A suitable catalyst should have the ability to be activated and reused in the desired reaction. Therefore, the biocatalyst used in this synthetic reaction was activated and reused after the completion of the reaction (Figure 7). To

activate the TLL@MMI, first, the TLL@MMI used in the reaction was separated by centrifugation. Then, it was washed three times with ethanol and phosphate buffer at pH 8.5. Finally, it was dried for 3 h in a vacuum system at room temperature. The recovered biocatalyst was used five times in the pyrazole synthesis reaction. After the end of the fifth cycle (after using the biocatalyst for 40 h), it still has 53% activity.

CONCLUSIONS

In conclusion, we have designed an easy-process, multi-component enzyme-catalyzed system for the synthesis of

Scheme 2. Proposed Mechanism

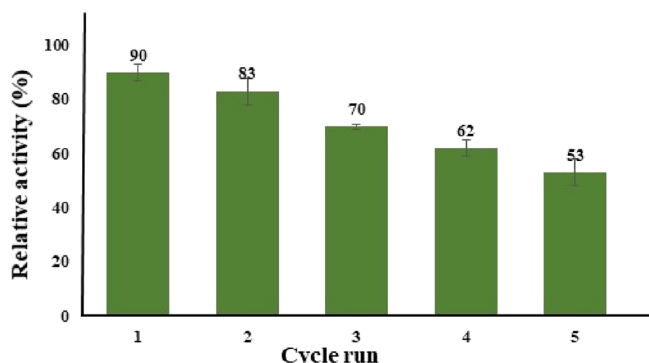
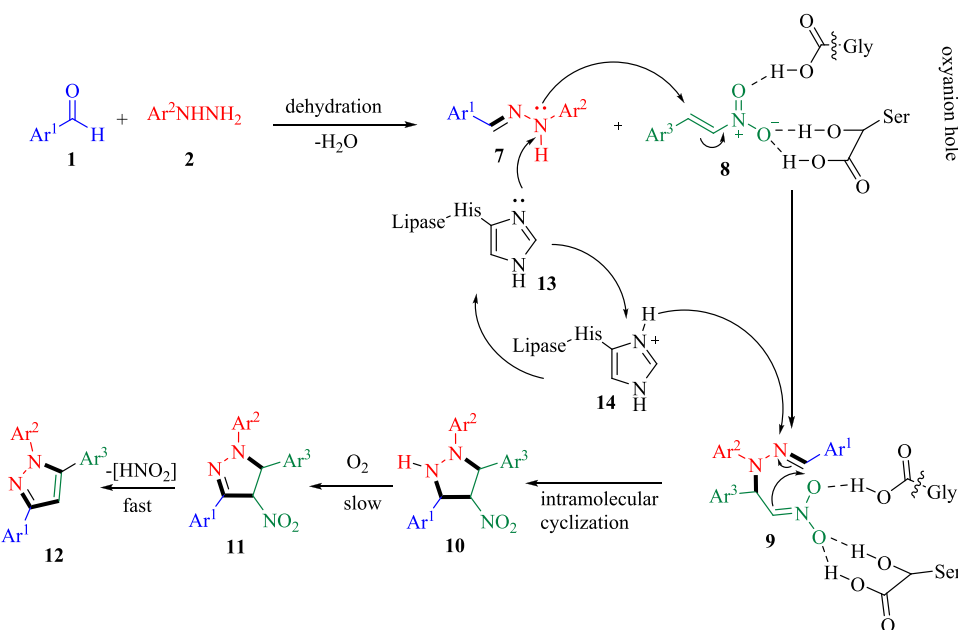


Figure 7. Reusability of the TLL@MMI catalyst in the pyrazole synthesis reaction.

1,3,5-trisubstituted pyrazole derivatives. All materials were added simultaneously at the beginning of the reaction. Various lipases were investigated; the TLL@MMI, immobilized *T. lanuginosus* lipase (TLL) on multivariate of MOF-5/IRMOF-3 (MMI), showed the best performance. Finally, this biocatalyst was examined after the reaction by FTIR, XRD, SEM, and solvent and thermal stability tests, and its stability was confirmed.

ASSOCIATED CONTENT

Supporting Information

The Supporting Information is available free of charge at <https://pubs.acs.org/doi/10.1021/acsomega.3c09875>.

Experimental section; characterization data of compounds 4a–p; and ^1H NMR, ^{13}C NMR, and mass spectra of the products (PDF)

AUTHOR INFORMATION

Corresponding Author

Zohreh Habibi – Department of Organic Chemistry, Faculty of Chemistry, Shahid Beheshti University, Tehran 1983969411,

Iran; orcid.org/0000-0002-0407-1469;
Email: Z_habibi@sbu.ac.ir

Authors

Zeynab Rangraz – Department of Organic Chemistry, Faculty of Chemistry, Shahid Beheshti University, Tehran 1983969411, Iran; orcid.org/0009-0002-5663-5024

Mostafa M. Amini – Department of Inorganic Chemistry, Faculty of Chemistry, Shahid Beheshti University, Tehran 1983963113, Iran; orcid.org/0000-0003-2974-1024

Complete contact information is available at:
<https://pubs.acs.org/10.1021/acsomega.3c09875>

Notes

The authors declare no competing financial interest.

ACKNOWLEDGMENTS

This research was financially supported by Shahid Beheshti University of Tehran, to which the authors are thankful.

REFERENCES

- Guo, Y.; Wang, G.; Wei, L.; Wan, J.-P. Domino C–H Sulfenylation and pyrazole Annulation for Fully Substituted pyrazole Synthesis in Water Using Hydrophilic Enaminones. *Journal of Organic Chemistry* **2019**, *84* (5), 2984–2990.
- Jacoby, R. F.; Seibert, K.; Cole, C. E.; Kelloff, G.; Lubet, R. A. The Cyclooxygenase-2 Inhibitor Celecoxib Is a Potent Preventive and Therapeutic Agent in the Min Mouse Model of Adenomatous Polyposis1. *Cancer Res.* **2000**, *60* (18), 5040–5044.
- Friedrich, G.; Rose, T.; Rissler, K. Determination of Isoniazid and its hydroxy and O-sulfated metabolites by on-line sample preparation liquid chromatography with fluorescence detection. *Journal of Chromatography B* **2002**, *766* (2), 295–305.
- Tsutomu, K.; Toshitaka, N. Effects of 1,3-diphenyl-5-(2-dimethylaminopropionamide)-pyrazole[difenamizole] on a conditioned avoidance response. *Neuropharmacology* **1978**, *17* (4), 249–256.
- Calvello, R.; Panaro, M. A.; Carbone, M. L.; Cianciulli, A.; Perrone, M. G.; Vitale, P.; Malerba, P.; Scilimati, A. Novel selective COX-1 inhibitors suppress neuroinflammatory mediators in LPS-stimulated N13 microglial cells. *Pharmacol. Res.* **2012**, *65* (1), 137–148.

(6) Fowler, S. W.; Walker, J. M.; Klakotskaia, D.; Will, M. J.; Serfozo, P.; Simonyi, A.; Schachtman, T. R. Effects of a metabotropic glutamate receptor 5 positive allosteric modulator, CDPPB, on spatial learning task performance in rodents. *Neurobiology of Learning and Memory* **2013**, *99*, 25–31.

(7) Rostami, H.; Shiri, L.; Khani, Z. Recent advances in the synthesis of pyrazole scaffolds via nanoparticles: A review. *Tetrahedron* **2022**, *110*, No. 132688.

(8) Karrouchi, K.; Radi, S.; Ramli, Y.; Taoufik, J.; Mabkhot, Y.; Alaizari, F.; Ansar, M. Synthesis and Pharmacological Activities of pyrazole Derivatives: A Review. *Molecules* **2018**, *23*, 134 DOI: [10.3390/molecules23010134](https://doi.org/10.3390/molecules23010134).

(9) Bennani, F. E.; Doudach, L.; Cherhah, Y.; Ramli, Y.; Karrouchi, K.; Ansar, M. h.; Faouzi, M. E. A. Overview of recent developments of pyrazole derivatives as an anticancer agent in different cell line. *Bioorganic Chemistry* **2020**, *97*, No. 103470.

(10) Ansari, A.; Ali, A.; Asif, M.; Shamsuzzaman, S. Biologically active pyrazole derivatives. *New J. Chem.* **2017**, *41* (1), 16–41.

(11) Fustero, S.; Sánchez-Roselló, M.; Barrio, P.; Simón-Fuentes, A. From 2000 to Mid-2010: A Fruitable Decade for the Synthesis of Pyrazoles. *Chem. Rev.* **2011**, *111* (11), 6984–7034.

(12) Aldulaijan, S.; Nabil, S.; Alharthi, S.; Abdullatif, B. A. L.; Abdel-Naby, A. S. Use of a bioresource nanocomposite as a heterogeneous base catalyst for the green synthesis of novel bioactive pyrazoles: antibacterial evaluation using molecular docking. *New J. Chem.* **2023**, *47* (28), 13367–13377.

(13) Singh, S.; Yadav, S.; Minakshi, M.; Pundeer, R. Green Synthesis of Pyrazoles: Recent Developments in Aqueous Methods. *SynOpen* **2023**, *07* (03), 297–312.

(14) Corradi, A.; Leonelli, C.; Rizzuti, A.; Rosa, R.; Veronesi, P.; Grandi, R.; Baldassari, S.; Villa, C. New “Green” Approaches to the Synthesis of pyrazole Derivatives. *Molecules* **2007**, *12*, 1482–1495.

(15) Climent, M. J.; Corma, A.; Iborra, S. Homogeneous and heterogeneous catalysts for multicomponent reactions. *RSC Adv.* **2012**, *2* (1), 16–58.

(16) Dömling, A.; Wang, W.; Wang, K. Chemistry and Biology Of Multicomponent Reactions. *Chem. Rev.* **2012**, *112* (6), 3083–3135.

(17) Ishwar Bhat, S. One-Pot Construction of Bis-Heterocycles through Isocyanide Based Multicomponent Reactions. *ChemistrySelect* **2020**, *5* (27), 8040–8061.

(18) Li, M.-M.; Huang, H.; Tian, W.; Pu, Y.; Zhang, C.; Yang, J.; Ren, Q.; Tao, F.; Deng, Y.; Lu, J. Construction of multi-substituted pyrazoles via potassium carbonate-mediated [3+ 2] cycloaddition of in situ generated nitrile imines with cinnamic aldehydes. *RSC Adv.* **2022**, *12* (21), 13087–13092.

(19) Fan, X.-W.; Lei, T.; Zhou, C.; Meng, Q.-Y.; Chen, B.; Tung, C.-H.; Wu, L.-Z. Radical Addition of hydrazones by α -Bromo Ketones To Prepare 1,3,5-Trisubstituted Pyrazoles via Visible Light Catalysis. *Journal of Organic Chemistry* **2016**, *81* (16), 7127–7133.

(20) Deng, X.; Mani, N. S. Reaction of N-Monosubstituted hydrazones with Nitroolefins: A Novel Regioselective pyrazole Synthesis. *Org. Lett.* **2006**, *8* (16), 3505–3508.

(21) Shi, C.; Ma, C.; Ma, H.; Zhou, X.; Cao, J.; Fan, Y.; Huang, G. Copper-catalyzed synthesis of 1,3,4-trisubstituted and 1,3,4,5-tetrasubstituted pyrazoles via [3 + 2] cycloadditions of hydrazones and nitroolefins. *Tetrahedron* **2016**, *72* (27), 4055–4058.

(22) Pal, G.; Paul, S.; Ghosh, P. P.; Das, A. R. PhIO promoted synthesis of nitrile imines and nitrile oxides within a micellar core in aqueous media: a regiocontrolled approach to synthesizing densely functionalized pyrazole and isoxazoline derivatives. *RSC Adv.* **2014**, *4* (16), 8300–8307.

(23) da Silva, J. L.; Sales, M. B.; de Castro Bizerra, V.; Nobre, M. M.; de Sousa Braz, A. K.; da Silva Sousa, P.; Cavalcante, A. L. G.; Melo, R. L. F.; De Sousa Junior, P. G.; Neto, F. S.; et al. Lipase from *Yarrowia lipolytica*: Prospects as an Industrial biocatalyst for Biotechnological Applications. *Fermentation* **2023**, *9*, 581 DOI: [10.3390/fermentation9070581](https://doi.org/10.3390/fermentation9070581).

(24) Melo, R. L. F.; Sales, M. B.; de Castro Bizerra, V.; de Sousa Junior, P. G.; Cavalcante, A. L. G.; Freire, T. M.; Neto, F. S.; Bilal, M.; Jesionowski, T.; Soares, J. M.; et al. Recent applications and future prospects of magnetic biocatalysts. *Int. J. Biol. Macromol.* **2023**, *253*, No. 126709.

(25) Das, S.; Zhao, L.; Elofson, K.; Finn, M. G. Enzyme Stabilization by Virus-Like Particles. *Biochemistry* **2020**, *59* (31), 2870–2881.

(26) Rodrigues, A. F. S.; da Silva, A. F.; da Silva, F. L. B.; dos Santos, K. M.; de Oliveira, M. P.; Nobre, M. M. R.; Catumba, B. D.; Sales, M. B.; Silva, A. R. M.; Braz, A. K. S.; et al. A scientometric analysis of research progress and trends in the design of laccase biocatalysts for the decolorization of synthetic dyes. *Process Biochemistry* **2023**, *126*, 272–291.

(27) Datta, S.; Christena, L. R.; Rajaram, Y. R. S. Enzyme immobilization: an overview on techniques and support materials. *3 Biotech* **2013**, *3* (1), 1–9.

(28) Pérez-Tomás, J. Á.; Brucato, R.; Griffin, P.; Kostal, J.; Brown, G.; Mix, S.; Marr, P. C.; Marr, A. C. Entrapment in Hydril gels: Hydro-Ionic Liquid polymer gels for enzyme immobilization. *Catal. Today* **2024**, *432*, No. 114595.

(29) Lian, X.; Fang, Y.; Joseph, E.; Wang, Q.; Li, J.; Banerjee, S.; Lollar, C.; Wang, X.; Zhou, H.-C. Enzyme–MOF (metal–organic framework) composites. *Chem. Soc. Rev.* **2017**, *46* (11), 3386–3401.

(30) Silva, A. R. M.; Alexandre, J. Y. N. H.; Souza, J. E. S.; Neto, J. G. L.; de Sousa Júnior, P. G.; Rocha, M. V. P.; dos Santos, J. C. S. The Chemistry and Applications of Metal–Organic Frameworks (MOFs) as Industrial Enzyme Immobilization Systems. *Molecules* **2022**, *27*, 4529 DOI: [10.3390/molecules27144529](https://doi.org/10.3390/molecules27144529).

(31) Xie, W.; Zang, X. Lipase immobilized on ionic liquid-functionalized magnetic silica composites as a magnetic biocatalyst for production of trans-free plastic fats. *Food Chem.* **2018**, *257*, 15–22.

(32) Ren, S.; Wang, F.; Gao, H.; Han, X.; Zhang, T.; Yuan, Y.; Zhou, Z. Recent Progress and Future Prospects of Laccase Immobilization on MOF Supports for Industrial Applications. *Appl. Biochem. Biotechnol.* **2023**, *1669* DOI: [10.1007/s12010-023-04607-6](https://doi.org/10.1007/s12010-023-04607-6).

(33) Sales, M. B.; Neto, J. G.; De Sousa Braz, A. K.; De Sousa Junior, P. G.; Melo, R. L.; Valério, R. B.; Serpa, J. D.; Da Silva Lima, A. M.; De Lima, R. K.; Guimaraes, A. P.; et al. Trends and Opportunities in Enzyme Biosensors Coupled to Metal-Organic Frameworks (MOFs): An Advanced Bibliometric Analysis. *Electrochim* **2023**, *4*, 181–211.

(34) Brahmachari, G. Chapter 13 - Lipase-catalyzed organic transformations: a recent update. In *Biotechnol. Microbial Enzymes* (Second Edition), Academic Press, 2023; pp 297–321.

(35) Gupta, R. D. Recent advances in enzyme promiscuity. *Sustainable Chemical Processes* **2016**, *4* (1), 2.

(36) Kapoor, M.; Gupta, M. N. Lipase promiscuity and its biochemical applications. *Process Biochemistry* **2012**, *47* (4), 555–569.

(37) Kowalczyk, P.; Koszelewski, D.; Gawdzik, B.; Samsonowicz-Górski, J.; Kramkowski, K.; Wypych, A.; Lizut, R.; Ostaszewski, R. Promiscuous Lipase-Catalyzed Markovnikov Addition of H-Phosphites to Vinyl Esters for the Synthesis of Cytotoxic α -Acyloxy Phosphonate Derivatives. *Materials* **2022**, *15* (5), 1975.

(38) Samsonowicz-Górski, J.; Koszelewski, D.; Kowalczyk, P.; Śmigielski, P.; Hrunyk, A.; Kramkowski, K.; Wypych, A.; Szymczak, M.; Lizut, R.; Ostaszewski, R. Promiscuous Lipase-Catalyzed Knoevenagel–Phospha–Michael Reaction for the Synthesis of Antimicrobial β -Phosphono Malonates. *Int. J. Mol. Sci.* **2022**, *23* (15), 8819.

(39) Patti, A.; Sanfilippo, C. Stereoselective Promiscuous Reactions Catalyzed by Lipases. *International Journal of Molecular Sciences* **2022**, *23* (5), 2675.

(40) Dwivedee, B. P.; Soni, S.; Sharma, M.; Bhaumik, J.; Laha, J. K.; Banerjee, U. C. Promiscuity of Lipase-Catalyzed Reactions for Organic Synthesis: A Recent Update. *ChemistrySelect* **2018**, *3* (9), 2441–2466.

(41) Koszelewski, D.; Ostaszewski, R. Biocatalytic Promiscuity of Lipases in Carbon-Phosphorus Bond Formation. *ChemCatChem* **2019**, *11* (10), 2554–2558.

(42) Deng, H.; Doonan, C. J.; Furukawa, H.; Ferreira, R. B.; Towne, J.; Knobler, C. B.; Wang, B.; Yaghi, O. M. Multiple Functional Groups of Varying Ratios in Metal-Organic Frameworks. *Science* **2010**, *327* (5967), 846–850.

(43) Li, J.; Wang, Y.; Yu, Y.; Li, Q. Functionality proportion and corresponding stability study of multivariate metal-organic frameworks. *Chin. Chem. Lett.* **2018**, *29* (6), 837–841.

(44) Bai, W.; Li, S.; Ma, J.; Cao, W.; Zheng, J. Ultrathin 2D metal-organic framework (nanosheets and nanofilms)-based x D–2D hybrid nanostructures as biomimetic enzymes and supercapacitors. *Journal of Materials Chemistry A* **2019**, *7* (15), 9086–9098.

(45) Hu, C.; Bai, Y.; Hou, M.; Wang, Y.; Wang, L.; Cao, X.; Chan, C. W.; Sun, H.; Li, W.; Ge, J.; Ren, K. Defect-induced activity enhancement of enzyme-encapsulated metal-organic frameworks revealed in microfluidic gradient mixing synthesis. *Sci. Adv.* **2020**, *6* (5), No. eaax5785.

(46) Mehta, J.; Dhaka, S.; Bhardwaj, N.; Paul, A. K.; Dayananda, S.; Lee, S.-E.; Kim, K.-H.; Deep, A. Application of an enzyme encapsulated metal-organic framework composite for convenient sensing and degradation of methyl parathion. *Sens. Actuators, B* **2019**, *290*, 267–274.

(47) Sabouni, R.; Kazemian, H.; Rohani, S. A novel combined manufacturing technique for rapid production of IRMOF-1 using ultrasound and microwave energies. *Chemical Engineering Journal* **2010**, *165* (3), 966–973.

(48) Xing, X.; Jia, J.-Q.; Zhang, J.-F.; Zhou, Z.-W.; Li, J.; Wang, N.; Yu, X.-Q. CALB immobilized onto magnetic nanoparticles for efficient kinetic resolution of racemic secondary alcohols: long-term stability and reusability. *Molecules* **2019**, *24* (3), 490.

(49) Cassimjee, K. E.; Kourist, R.; Lindberg, D.; Wittrup Larsen, M.; Thanh, N. H.; Widersten, M.; Bornscheuer, U. T.; Berglund, P. One-step enzyme extraction and immobilization for biocatalysis applications. *Biotechnology Journal* **2011**, *6* (4), 463–469.

(50) Poojari, Y.; Clarsen, S. J. Thermal stability of *Candida antarctica* lipase B immobilized on macroporous acrylic resin particles in organic media. *Biocatalysis and Agricultural Biotechnology* **2013**, *2* (1), 7–11.

(51) Costa, I. O.; Rios, N. S.; Lima, P. J. M.; Gonçalves, L. R. B. Synthesis of organic-inorganic hybrid nanoflowers of lipases from *Candida antarctica* type B (CALB) and *Thermomyces lanuginosus* (TLL): Improvement of thermal stability and reusability. *Enzyme Microb. Technol.* **2023**, *163*, No. 110167.

(52) Deng, X.; Mani, N. S. Regioselective Synthesis of 1,3,5-Tri- and 1,3,4,5-Tetrasubstituted Pyrazoles from N-Arylhydrazones and Nitroolefins. *Journal of Organic Chemistry* **2008**, *73* (6), 2412–2415.

(53) Wang, Y.; Wang, N. Hydrolase-Catalyzed Promiscuous Reactions and Applications in Organic Synthesis. In *Molecular Biotechnology*, IntechOpen, 2019.

(54) Li, F.; Xu, Y.; Wang, C.; Wang, C.; Xie, H.; Xu, Y.; Chen, P.; Wang, L. Efficient synthesis of substituted pyrazoles Via [3 + 2] cycloaddition catalyzed by lipase in ionic liquid. *Process Biochemistry* **2023**, *124*, 253–258.